NASA-CR-200941

An annual report for

STUDIES OF DISKS AROUND THE SUN AND OTHER STARS

NASA Grant No.: NAGW-4468

SwRI Project No.: 15-7238

Submitted by:

Dr. S. Alan Stern, Principal Investigator
Space Sciences Division
Southwest Research Institute
Boulder, Colorado 80302

1 January 1996

INTRODUCTION

This is the January 1996 Annual report for NAGW-4468 (SwRI Project 15-7238), *Studies of Disks Around the Sun and Other Stars,* (S.A. Stern, PI).

We are conducting research designed to enhance our understanding of the evolution and detectability of comet clouds and disks. This area holds promise for also improving our understanding of outer solar system formation, the bombardment history of the planets, the transport of volatiles and organics from the outer solar system to the inner planets, and to the ultimate fate of comet clouds around the Sun and other stars. According to "standard" theory, both the Kuiper Disk and the Oort Cloud are (at least in part) natural products of the planetary accumulation stage of solar system formation. One expects such assemblages to be a common attribute of other solar systems. Therefore, searches for comet disks and clouds orbiting other stars offer a new method for inferring the presence of planetary systems.

This two-element program consists modeling collisions in the Kuiper Disk and the dust disks around other stars. The modeling effort focuses on moving from our simple, first-generation, Kuiper disk collision rate model, to a time-dependent, second-generation model that incorporates physical collisions, velocity evolution, dynamical erosion, and various dust transport mechanisms. This second generation model will be used to study the evolution of surface mass density and the object-size spectrum in the disk. The observational effort focuses on obtaining submm/mm-wave flux density measurements of 25-30 IR excess stars in order to better constrain the masses, spatial extent, and structure of their dust ensembles.

RECENT PROGRESS

1) We have now completed the first model of collision rates of the Kuiper Disk. With this model we explored the rate of collisions among bodies in the present-day Kuiper Disk as a function of the total mass and population size structure of the Disk. We find that collisional evolution is an important evolutionary process in the Disk as a whole, and indeed, that it is likely the dominant evolutionary process beyond $\approx$ 42 AU, where dynamical instability timescales exceed the age of the solar system. Two key findings we report from this modelling work are: (i) That unless the Disk's population structure is sharply truncated for radii smaller than $\sim$1-2 km, collisions between comets and smaller debris are occurring so frequently in the Disk, and with high enough velocities, that the small body (i.e., km-class object) population in the disk has probably developed into a collisional cascade, thereby implying that the Kuiper Disk comets may not all be primordial, and (ii) that the rate of collisions of smaller bodies with larger $100 < R < 400$ km objects (like 1992QB$_1$ and its cohorts) is so low that there appears to be a dilemma in explaining how QB$_1$s could have grown by binary accretion in the disk as we know it. Given these findings, it appears that either the present-day paradigm for the formation of Kuiper Disk is failed in some fundamental respect, or that the present-day disk is no longer representative of the ancient structure from which it evolved. In particular, it appears that the 30-50 AU region of the Kuiper Disk has very likely

experienced a strong decrease in its surface mass density over time. This in turn suggests the intriguing possibility that the present-day Kuiper Disk evolved through a more erosional stage reminiscent of the disks around the A-stars β Pictorus, α PsA, and α Lyr. These results were published in *The Astronomical Journal* this year.

2) We have also used this model and a second code to estimate the detectability of IR emission from debris created by collisions. We found that eccentricities in the Kuiper Disk are high enough to promote erosion on virtually all objects up to $\sim$ 30 km, independent of their impact strength. Larger objects, such as the 50-170 km radius "QB_1" population, will suffer net erosion if their orbital eccentricity is greater than ≈ 0.05 (≈ 0.1) if they are structurally weak (strong). The model predicts a net collisional erosion rate from all objects out to 50 AU ranging from 3×10^{16} to 10^{19} g yr,$^{-1}$ depending on the mass, population structure, and mechanical properties of the objects in the Disk. We find two kinds of collisional signatures that this debris should generate. First, there should be a relatively smooth, quasi-steady-state, longitudinally isotropic, far IR (i.e, $\sim$ 60 μm peak) emission near the ecliptic in the solar system's invariable plane ecliptic, caused by debris created by the ensemble of ancient collisions. The predicted optical depth of this emission could be as low as 7×10^{-8}, but is most likely between 3×10^{-7} and 5×10^{-6}. We find that this signature was most likely below IRAS detection limits, but that it should be detectable by both ISO and SIRTF. Second, very recent impacts in the disk should produce short-lived, discrete clouds with significantly enhanced, localized IR emission signatures superimposed on the smooth, invariable plane emission. These discrete clouds should have angular diameters up to 0.2 deg, and annual parallaxes up to 2.6 deg. Individual expanding clouds (or trails) should show significant temporal evolution over timescales of a few years. As few as zero or as many as several 10^2 such clouds may be detectable in a complete ecliptic survey at ISO's sensitivity, depending on the population structure of the Kuiper Disk. This work was recently accepted for publication in *Astronomy & Astrophysics.*

3) We then emplyed our model to study the collisional environment in the ancient Kuiper Disk. We explored the consequences of a massive, primordial Kuiper Disk using a collision rate model that assumes the dominant growth mechanism in the 35-50 AU region was pairwise accretion. We found that the growth of QB_1-class objects from seeds only kilometers in diameter required a very low eccentricity environment, with mean random eccentricities of order 1% or less. Duncan et al. (1995) have shown that the presence of Neptune induces characterstic eccentricities throughout the 30-50 AU region of a few percent or greater. We therefore concluded that growth of objects in the 30 to 50 AU zone to a least this size must have occurred before Neptune reached a fraction of its final mass. Once Neptune grew sufficiently to induce eccentricities exceeding $\approx$1%, we found that the disk environment became highly erosive for objects with radii smaller than $\sim$20–30 kilometers, which likely created a flattening in the disk's population power law slope between radius scales of $\approx$30 to $\approx$100 km, depending on the density and strength of such objects. This erosive environment could have resulted in sufficient mass depletion to evolve the disk to its present, low-mass state, independent of dynamical losses (which surely also played an important role). During the period of rapid erosive mass loss, the disk probably exhibited optical depths of 10^{-4} to 10^{-5} (reminiscent

of β Pictoris), for a timescale of $\sim 10^7$ to $\sim 10^8$ years. As a result of the evolution of the disk inside 50 AU, we suggested that (i) the present-day Solar System's surface mass density edge near 30 AU is actually only the inner edge of a surface mass density *trough*, and (ii) that the surface mass density of solids may rise back beyond $\sim$50 AU, where the giant planets have never induced erosive high eccentricities. Indeed, the growth of objects in the region beyond 50 AU may be continuing to the present. This work was submitted for publication to *The Astronomical Journal.*

These three papers were also accompanied by an invited review, submitted to the *Planetary Ices* book, summarizing the present state of knowledge about the Kuiper Disk and Pluto. PI Stern also wrote a popular-level article on extra-solar comets for *Astronomy* magazine.

4) Additionally, PI Stern gave three invited talks summarizing the collisional modelling results obtained under the Origins program. A list of these invited talks is attached.

5) Finally, in July 1995, we organized and sponsored a 2-day workshop on collisions in the Kuiper Disk. This workshop was attended by D. Davis (PSI), P. Farinella (Italy), R. Canup (U. Colorado), M. Festou (France), J. Colwell (U. Colorado), H. Levison (SwRI), and PI Stern (SwRI). The proceedings of this workshop were informally published and the distributed among the participants. A copy was also sent to Origins program scientist Trish Rogers.

6) For 1996 we plan to construct the time-dependent collision code described in our Origins proposal, and to begin exploiting it to better understand the growth of objects in the Kuiper Disk.

RELEVANT PUBLICATIONS

Collision Rates in the Kuiper Disk and Their Implications. S.A. Stern, *The Astronomical Journal*, **110**, 856, 1995.

Pluto and the Kuiper Disk. S.A. Stern. "Ices in the Solar System." (C. DeBergh, B. Schmitt, M.C. Festou, eds.), in press 1996.

Signatures of Collisions in the Kuiper Disk. S.A. Stern. *Astronomy & Astrophysics*, in press, 1996.

On the Origin of Pluto, Charon, and the Pluto-Charon Binary. S.A. Stern, W.B. McKinnon, and J.I. Lunine. Invited chapter for the UA Press Space Science Series volume, "Pluto & Charon," in press, 1996.

The Collisional Environment, Timescales, and Architecture of the Ancient, Massive Kuiper Disk. Stern, S.A.. Submitted to the Astronomical Journal.

Interstellar Intruders. S.A. Stern, Astronomy Magazine, in press for 1996.

1995 SCIENTIFIC PRESENTATIONS & ABSTRACTS

Collisions in the Kuiper Disk. Astronomy Luncheon Seminar. Queen's University Department of Physics. Kingston, Ontario, 2 February 1995.

Pluto, Charon, and The Kuiper Disk. Ices in the Solar System Meeting. Toulouse, France, 25 March 1995.

The Kuiper Disk: Evidence for Arrested Planetary Accretion? Laboratory for Atmospheric and Space Physics Seminar, University of Colorado, Boulder, CO, 28 September 1995.

On The Collisional Environment, Accretion Timescales, And Architecture of The Massive, Primordial Kuiper Disk

S. Alan Stern
Geophysical, Astrophysical, & Planetary Sciences
Space Science Department
Southwest Research Institute
Boulder, CO 80302 USA

13 Manuscript Pages
05 Figures

Submitted to *The Astronomical Journal:* 04 December 1995
Revised: 02 April 1996

Running Title: The Ancient Kuiper Disk

S. Alan Stern
Space Science Department
Southwest Research Institute
1050 Walnut Street, Suite 429
Boulder, CO 80302

[303] 546-9670 (voice)
[303] 546-9687 (fax)

alan@everest.space.swri.edu

Abstract

Previous collisional modelling has suggested that the mass of the primordial Kuiper Disk between 30 and 50 AU was probably of order $10M_\oplus$ to $50M_\oplus$. We explore the consequences of a massive, primordial Kuiper Disk using a collision rate model that assumes the dominant growth mechanism in the 35-50 AU region was pairwise accretion. We find that the growth of QB_1-class objects from seeds only kilometers in diameter required a very low eccentricity environment, with mean random eccentricities of order 1% or less. Duncan et al. (1995) have shown that the presence of Neptune induces characterstic eccentricities throughout the 30-50 AU region of a few percent or greater. We therefore conclude that growth of objects in the 30 to 50 AU zone to a least this size must have occurred before Neptune reached a fraction of its final mass. Once Neptune grew sufficiently to induce eccentricities exceeding $\approx$1%, we find that the disk environment became highly erosive for objects with radii smaller than $\sim$20–30 kilometers, which likely created a flattening in the disk's population power law slope between radius scales of $\approx$30 to $\approx$100 km, depending on the density and strength of such objects. This erosive environment could have resulted in sufficient mass depletion to evolve the disk to its present, low-mass state, independent of dynamical losses (which surely also played an important role). During the period of rapid erosive mass loss, the disk probably exhibited optical depths of 10^{-4} to 10^{-5} (reminiscent of β Pictoris), for a timescale of $\sim 10^7$ to $\sim 10^8$ years. As a result of the evolution of the disk inside 50 AU, we suggest that (i) the present-day Solar System's surface mass density edge near 30 AU is actually only the inner edge of a surface mass density *trough*, and (ii) that the surface mass density of solids may rise back beyond $\sim$50 AU, where the giant planets have never induced erosive high eccentricities. Indeed, the growth of objects in the region beyond 50 AU may be continuing to the present; the exploration of this region is encouraged.

1. Introduction

Almost a half-century ago, Edgeworth (1949) and Kuiper (1951) made prescient predictions that the Sun should be surrounded by a disk-like ensemble of comets and other "debris" located beyond the orbit of Neptune. The case for such a reservoir was strengthened when it was later pointed out that such a disk would be an efficient source region from which to derive the short-period comets (Fernández 1980). Convincing dynamical simulations supporting this link between the Jupiter Family comets and the Kuiper Disk region arose when Duncan et al. (1988) and later Quinn et al. (1990) showed that a low-inclination source region appears required to explain the low-inclination orbit distribution of the Jupiter Family comets.

Observational confirmation of the Kuiper Disk was first achieved with the discovery of object 1992QB$_1$ by Jewitt & Luu (1993). As of mid-1996, no fewer than 32 QB$_1$-like, trans-Neptunian objects have been discovered (cf., Jewitt & Luu 1995, and Weissman 1995 for background). Based on the detection statistics obtained to date, one can easily estimate that a complete ecliptic survey would reveal $\sim 3.5 \times 10^4$ such bodies orbiting between $\approx$30 and 50 AU. These icy outer Solar System bodies are expected to have dark surfaces consisting of an icy matrix contaminated by silicates and organics (e.g., Cruikshank 1994). Assuming a typical geometric albedo of 4%, and the absence of coma, the distances and magnitudes of these objects indicate they have radii between roughly 50 and 180 km. The discovery of such large objects implies that widescale accretion took place in the 30 to 50 AU zone.

In addition to the larger, QB$_1$-like bodies, dynamical modelling by Duncan et al. (1995) predicts up to $\sim 10^{10}$ 1 to 6 km radius comets are required in this region to satisfy the short-period comet flux. Recently, Cochran et al. (1995a,b) have reported Hubble Space Telescope (HST) observations giving direct evidence of objects in or near this size class.

Several facts regarding the population of objects discovered to date are relevant to what follows. First, work by various modelling teams (e.g., Duncan et al. 1995) has convincingly shown that the objects being discovered in the Kuiper Disk reside in long-lived dynamical reservoirs; as such, it is accepted that the objects we detect were formed in the disk. Second, the estimated total mass of the entire disk population interior to 50 AU, from comets upward, is of order 0.1-0.4$M_\oplus$ (Weissman & Levison 1996). Third, about 60% of the QB$_1$s discovered to date appear to be in mean motion resonance with

Neptune and exhibit eccentricities near 25% and inclinations of 15-30 degrees; those QB_1s that do not appear to be in mean motion resonances exhibit characteristic eccentricities and inclinations of <10% and <10 degrees. Fourth, most QB_1s have been discovered either in the 3:2 Neptune resonance or beyond 42 AU, where orbits are stable for longer than the age of the Solar System.

With the rapid pace of observational advances concerning the population structure of the Kuiper Disk, it has now become feasible to construct models to evaluate the collisional properties of the Kuiper Disk. An extensive study of collision rate dependencies in the *present-day* Kuiper Disk was recently published by this author (Stern 1995; hereafter Paper I). Additional collisional-environment studies have been reported in an abstract by Young & Asphaug (1995) and a complete manuscript by Davis & Farinella (1996). Work to evaluate the IR signatures that the present-day disk should generate has been published by Backman et al. (1995) and Stern (1996); there is also an unpublished manuscript by Alcock & Hut (1995) on the possible detectability of optical flashes from comet-comet collisions in the Kuiper Disk.

A major result obtained from the collisional modelling reported in Paper I was that the total rate of collisions of smaller bodies with QB_1-class objects is so low that it creates a dilemma in explaining how QB_1s could have grown by pairwise accretion in the present-day disk. Simply put, it implies that collisions appear to be too infrequent to accumulate QB_1-sized objects in the age of the Solar System. This in turn provides evidence that, unless large objects like the QB_1s were not built via a conventional aufbau (i.e., 'building up') process of pairwise accretion, then the internal random velocity and the mass of the disk have strongly evolved from its initial state. Other key results obtain from paper I are: (1) That present-day eccentricities in the disk preferentially promote erosion (i.e., net mass loss) over accumulation (i.e., net mass gain) for objects a few tens of kilometers in radius and smaller. (2) That unless the population of objects with radii of $\gtrsim$ 1 km was originally deficient, then the present-day population structure of the disk is involved in a collisional cascade; as such, most Kuiper Disk comets may not be structurally primordial. And (3), owing to the frequency and energetics of collisions between $\approx$1 to 6 km class and smaller bodies, a distinct change in slope in the population structure of the Kuiper Disk may have developed for objects with radii somewhere below $\sim$6 km. Many of these same conclusions were recently reached by Davis & Farinella (1996).

In Paper I it was suggested that the growth-time dilemma for QB_1 objects implies a far higher *primordial* disk mass, and that the present-day 30 to 50 AU zone is a highly-evolved, low-mass *remnant* of the initial structure. As such, it has become worthwhile to explore the collisional properties of such an earlier, high-mass structure.

That study is the subject of this paper. Our goals are to: (i) evaluate the rate of collisions in an early, massive Kuiper Disk; (ii) determine the growth and erosion times for objects in such a disk (whether growth or erosion predominates depends on the mean random eccentricities of the orbits in the disk); (iii) estimate the evolutionary timescales relevant to the growth of the larger bodies and the loss of mass as the disk evolved to its present state; and (iv) evaluate the implications of these findings for the architecture of the present-day disk.

2. The Early Collisional Environment

It is important to recognize that the consequences of collisions in the Kuiper Disk depend on whether the disk environment promotes net erosion or net accretion when collisions occur. Simply put, for an object of specified mechanical properties and mass, an analytical formalism can be derived (Stern 1996) to derive a critical collision velocity, or equivalently, a critical collision eccentricity e^*, above which impacts eject more mass from the object than the mass of the impactor, and below which the target body gains mass and thereby grows.

The results of such calculations are shown in Figure 1, which demonstrates that for strong objects (i.e., with strength like H_2O ice) that have roughly 10 km radii and smaller, where gravitational binding energy is not important, the mean disk eccentricity $\langle e \rangle$ must be < 0.01 to promote accretion. For weak objects (i.e., strength like snow) and radii of a few kilometers in radius or smaller, accretion requires $\langle e \rangle < 2 \times 10^{-3}$. For reference, $\langle e \rangle = 0.01$ corresponds to a characteristic collision speed of 87 m s^{-1} at 35 AU, and 66 m s^{-1} at 60 AU. The curves in Figure 1 also show that, for objects with radii exceeding roughly 5–15 kilometers, depending on their strength and density, gravitational binding energy begins to play an important role, making the objects more resistant to erosion. Concerning the QB_1 objects discovered to date, which are in the 100-170 km radius regime, the condition for sustained growth is $\langle e \rangle < 0.05 - 0.10$ if the objects are as strong as H_2O ice, and $\langle e \rangle < 0.02 - 0.05$ if they are mechanically weak like snow. Many of the detected objects have eccentricities that exceed these values of e*, and are therefore likely to be suffering erosion today.

Clearly, if a bottoms-up growth process from smaller to larger objects built up the QB_1s we observe in the disk, then the ancient disk must have maintained very low characteristic collision velocities (hence very low eccentricities) until objects grew to a size where they could withstand somewhat higher collision velocities. Since Neptune is the most likely source of the eccentricity growth that halted growth in the 30–50 AU region, it is likely that the growth from seeds a few kilometers in radius to at least the $\approx$20–30 km scale took place before Neptune became a significant perturber and introduced the erosive eccentricities observed today.

Once eccentricities increase to a few percent, objects from $\sim$30 km in radius upward to QB_1 scale can still grow, but significantly smaller objects will suffer mass loss through erosive collisions. Figure 2 presents estimates for the initial timescale for small objects to lose half their mass to erosive collisions, as a function of their eccentricity.

The top and bottom panels of Figure 2 show erosion timescale estimates for bodies with radii of 2.5 and 10 km, respectively. Even at $\langle e \rangle = 0.015$, the erosion timescales for 2.5 km radius objects are very short— 1×10^7 to 5×10^7 years at 35 and 45 AU, respectively. Objects with 10 km radii are expected to be eroded significantly on characteristic timescales of 3×10^7 to perhaps 1×10^8 years. Higher $\langle e \rangle$, weaker target bodies, and/or lower mean ejecta velocities will decrease these erosion timescales.

It is important to point out that this erosion timescale is not the timescale for objects to erode away, but simply the timescale for them to shrink significantly, which in turn causes their cross section for collisions to decrease. As this happens, the erosion timescale for a given object will lengthen. Also, as erosion through high-velocity collisions produces fine debris which will be radiation transported away, the mass of the disk will decline. As a result of these effects, collisionally-driven erosion tends to "self-regulate" itself. In the absence of sources (i.e., new objects being brought in), the remaining population will tend towards an erosion timescale like the length of time that has passed since erosion began. That is, the erosion timescale will tend to approach the age of the Solar System, which appears to be the case in the present-day disk (cf., Paper I).

3. Collision Rates in a Massive, Primordial Kuiper Disk

We have shown that the initial growth of the QB_1 population from kilometer-class seeds to objects with radii exceeding $\approx$20 km required very low mean random eccentricities in the disk, i.e., <0.005–0.01. We now turn to the growth timescales required to build the QB_1s, by deriving the timescale required for a given sized object to accrete its own mass (i.e., $T_{doubling}=m/\dot{m}$, where m is the starting mass and $\dot{m}$ is the rate at which mass impacts the object).

Our code for estimating collision rates in the Kuiper Disk was described in some detail in Paper I. This code is a simple, static multi-zone model for the computation of collision rates and instantaneous growth timescales. The model assumes that all growth takes place by binary accretion from small seed objects a few kilometers in scale. This code is useful for initial explorations such as those described below, but ultimately, a time-dependent code that includes coupled mass and velocity evolution, as well as run-away growth processes, must be applied. Such a code is now in development by this author and J. Colwell for application to the evolution of objects in the Kuiper Disk.

Briefly, the code defines the population in terms of a total mass and disk a power law exponent, α, on the size distribution of objects in the disk. Defined in this way, the number of objects $dN(r)$ between radius r and $r + dr$ is given by

$$dN(r) = N_0(r/r_0)^\alpha dr, \tag{1}$$

where N_0 is a normalization constant set by the estimated number of QB_1 objects in the 30 to 50 AU zone. We treat this size distribution as a series of monotonically increasing radius bins, with the objects in each successive bin a factor of 1.6 times larger in size (and thus 4 times higher in mass).

The code also defines a power law exponent β on the radial distribution of heliocentric surface mass density $\Sigma(R)$ in the disk, so that

$$\Sigma(R) = \Sigma_0(R/R_0)^\beta, \tag{2}$$

where Σ_0 is the normalization constant. For simplicity, we adopt a disk-wide $\langle i \rangle$ and $\langle e \rangle$ for each run. The assumption of a constant inclination throughout the disk implies an increasing scale height with heliocentric distance, which is a natural outcome if inclinations are set by mean random velocities equipartitioned between inclination and eccentricity. In what follows, we assume an equilibrium condition $\langle i \rangle = \frac{1}{2}\langle e \rangle$ between mean inclination and mean eccentricity (cf., Lissauer & Stewart 1993).

Once the global properties of the disk are defined as described above, we bin the disk into a series of radially-concentric tori that are 1 AU in width. For each size bin/heliocentric bin pair, the model computes the collision rate that a target of given size experiences from potential impactors in bins of equal or smaller size.

To compute collision rates for objects with orbits at each semi-major axis we adopt a particle in a box formalism. This approach states that the instantaneous collision rate c of target bodies with semimajor axis a, eccentricity e, and radius r_x being struck by impactors of radius r_y, is just:

$$\bar{c}(r_x, r_y, a, e, R) =$$

$$\sum_{R=a(1-\langle e\rangle)}^{a(1+\langle e\rangle)} \sqrt{\frac{GM_\odot}{4\pi^2 a^3}}\; T(a, \langle e\rangle, R)\; n(r_y, R)\; v_{xy}(a, \langle e\rangle, \langle i\rangle, R)\; \sigma_g(r_x, r_y, v_{xy}, v_{esc[x+y]}), \qquad (3)$$

where $T(a, \langle e\rangle, R)$ represents the time the target body in an orbit defined by $(a, \langle e\rangle, \langle i\rangle)$ spends at each distance R during its orbit. To compute $T(a, \langle e\rangle, R)$ we solve the central-field, Kepler time of flight equation explicitly for every $(a, \langle e\rangle)$ pair in the run's parameter space. The number density of impactors $n(r_y, R)$ in the torus centered at distance R is computed from the mass of the disk, the disk's wedge angle $\langle i\rangle$, its heliocentric population size structure power law (Eqn. 1), and its surface mass density power law (Eqn. 2). Here σ_g is the gravitational-focusing corrected collision cross section of the impactor+target pair. Gravitational focusing is important for targets roughly 50 km in size and larger, particularly in the case of low eccentricities (e.g., $\langle e\rangle < 10^{-2}$). Because the implicit assumption of a two-body encounter approximation in the gravitational scattering term of Eqn. (3) is not valid at very low eccentricities, this model is limited in the minimum mean random eccentricity for which valid results can be produced. For the largest objects we consider (162 km radius) this lower limit is $\langle e\rangle < 3 \times 10^{-4}$; for kilometer-class objects the code is valid down to $\langle e\rangle < 10^{-5}$. In what follows we will consider only disks with $\langle e\rangle > 10^{-3}$.

To calculate growth timescales we assume that every collision was completely inelastic. In reality, collisions will often result in some degree of mass loss. Still, so long as growth can proceed (i.e., $e<e^*$), this assumption is useful because it gives *lower limit* growth timescales.

The upper left panel in Figure 3 presents estimates of the *instantaneous* timescale for objects to double their mass by accretion, as a function of their size and heliocentric distance, assuming the mean disk eccentricity $\langle e \rangle = 3\times10^{-3}$; the upper right panel presents the same for a calculation for $\langle e \rangle$ near 3×10^{-2}. The corresponding lower panels in Figure 3 present the *integrated* timescales for objects to grow from 3 km seeds, as a function of their final size and their heliocentric distance. These curves were derived by integrating over the data in the upper panels of Figure 3 with respect to size.

The timescale estimates presented in Figure 3 reveal several important findings. First, consider a dynamically cold disk with $\langle e \rangle \approx 3 \times 10^{-3}$, so that 1–20 km radius bodies can grow (see Figure 1). The upper lefthand panel indicates that the growth times for QB_1-class objects in a low $\langle e \rangle$ environment are controlled in large part by the $\sim 3 \times 10^8$ year "growth barrier" required to grow objects about 30 km in radius from 3 km seeds. Once a threshold radius of about 20–30 km is reached, where gravitational focusing can play a signifcant role in increasing their accretional mass flux, objects begin to double in mass more and more quickly.

Unfortunately, even with $15M_\oplus$ of soids in the inner Kuiper Disk, the lower lefthand panel of Figure 3 shows that if $\langle e \rangle = 3 \times 10^{-3}$ in the 35–45 AU region, objects of QB_1-scale (i.e., 70-140 km in radius) required $\sim$2 Gyr to $\sim$6 Gyr to grow from 3 km radius seeds by strict binary accretion in the absence of gas. The growth timescales for QB_1-sized objects near 70 AU are about an order of magnitude longer still. As shown in the righthand panels of Figure 3, even if growth could occur at $\langle e \rangle = 2.5 \times 10^{-2}$, the estimated growth times in the Kuiper Disk far exceed the age of the Solar System for all objects with radii greater than $\approx$50 km. Changing the initial seed size from 3 km to 10 km does not significantly affect these results.

To achieve growth times of order 1 Gyr or less, which would be consistent with growth times for Neptune (cf., Lissauer et al. 1996), we must either (i) decrease $\langle e \rangle$ below 10^{-3} or (ii) increase the total mass inside 50 AU to 35–$50M_\oplus$, in which case $\langle e \rangle$ up to 6×10^{-3} can be allowed.† The increased disk mass is perhaps the more plausible alternative, particularly when one considers the fact that the equilibrium eccentricity that a population of 10 km radius comets will induce on itself at 45 AU can approach 10^{-3}, without any contribution from the giant planets or larger objects in the growing ensemble.

Figure 4 draws on the results of several dozen growth timescale calculations like those shown in Figure 3 to show how the growth times at 35 AU for 100 km radius QB_1s depend

† Alternatively, one could assume the initial seed size was much larger, say 100 km, invalidating the need for much growth by binary accretion.

on both the total disk mass in the 35 to 50 AU region and $\langle e \rangle$. For $35M_\oplus$ inside 50 AU, the estimated timescale to grow a 100 km radius QB_1 is near 0.4 Gyr for $\langle e \rangle = 10^{-3}$, 2.5 Gyr for $\langle e \rangle = 10^{-2}$, and 8 Gyr for $\langle e \rangle = 10^{-1}$. Increasing the disk mass inside 50 AU to a total of $50M_\oplus$ gives QB_1 growth timescales of 0.3 Gyr for $\langle e \rangle = 10^{-3}$, 2 Gyr for $\langle e \rangle = 10^{-2}$, and 6 Gyr for $\langle e \rangle = 10^{-1}$. As one might expect, the growth time decreases approximately linearly with mass for a fixed $\langle e \rangle$. Further, owing to the assumed lower number densities at greater distances from the Sun in this R^{-2} heliocentric surface mass density model, all the growth times increase by a factor of two by 45 AU.

The data in Figure 4 emphasize the importance of a dynamically cold disk for growing QB_1s. For example, to achieve the growth of QB_1s in under 1 Gyr, the disk must have remained very cold, of order $\langle e \rangle = 10^{-3}$. If $\langle e \rangle$ exceeded 2–3%, QB_1s cannot be grown from 3 km seeds in less than the age of the Solar System, even if there is 50 $M_\oplus$ of mass between 35 and 50 AU.

4. An Inferred Scenario for Kuiper Disk Evolution

The work presented above is a precursor to our development of time-dependent models to study accretion and erosion in the Kuiper Disk. However, from the results already obtained, it is possible to glean enough hints to suggest a scenario for growth in the region between about 30 and 50 AU.

Initially, the disk must have been dynamically quite cold to promote the growth of increasingly larger objects with time. Our growth timescale estimates indicate that the 100-170 km radius objects now present in great numbers may have grown from few kilometer radius seeds in as little as 500 million years, but more likely required 1 to 1.5 Gyr. Since objects in the 100-200 km radius regime will be be involved in runaway growth for characteristic disk orbit eccentricities below 1%, their growth had to be rapidly brought to a halt in order to prevent the widespread accretion of objects several times this size. We suspect therefore that growth was truncated when eccentricities were increased, probably due to the presence of Neptune, although internal perturbations in the disk is a plausible alternative.

The results derived above suggest that as eccentricities grew, they exceeded the critical eccentricity e^* boundary between growth and erosion for larger and larger scale objects. Once $e > 0.05$ to 0.01, it became possible for a rapid decrease in the number of objects with

$e^* < e$. The expectation is that this would cause the bulk of the small-body population to be rapidly eroded out "from under" the large-body population in a few times the characteristic erosion timescale. The effects of such erosion would be to significantly reduce the mass and increase the optical depth of the disk. By reducing the supply of impacting mass, the erosion of smaller objects would in turn significantly truncate the growth of larger bodies. It therefore appears that the largest objects in the present-day Kuiper Disk must have completed their growth within a few tens of millions of years of the time that eccentricities reached the 1% level, where the wholesale destruction of smaller bodies, from which they are built, would have sharply reduced the supply of material available to grow these QB_1s.

The results presented above also argue that, on a timescale of 10^7 to 10^8 years, collisional erosion would then whittle the disk mass down to $<<1M_\oplus$, producing characteristic mass loss rates of $\sim 10^{-6} M_\oplus$ to $\sim 10^{-7} M_\oplus$ yr^{-1}. Following the approach described in Stern (1996), we have calculated the characteristic radial optical depth generated by a $35M_\oplus$ disk of solids between 35 and 50 AU undergoing erosional mass loss. This model estimates the steady-state population balance between debris creation by collisions with the losses by radiation transport and gravitational dynamics. The optical depth computed by the model is the total optical depth for all objects from 3 μm dust to QB_1s.

The result of such a calculation is that a characteristic radial optical depth of $\approx 10^{-3}$ is found for $\langle e \rangle \approx 3 \times 10^{-3}$; the characteristic optical depths for $\langle e \rangle > 0.01$ are in the range 10^{-4} to 10^{-5}. These optical depths are 2 to 3 orders of magnitude higher than the optical depth predicted for the present-day disk (cf., Stern 1996), and are comparable to the present-day optical depth of the β Pic disk (cf., Backman & Paresce 1993). As such, the rapid evolution of our Kuiper Disk from its initial high-mass state to its present-day low-mass state suggested by this paper and others might have created a structure appearing similar in many respects to β Pictoris. Indeed, the β Pictoris system may now be presenting a Kuiper-like disk in transition from its initial high-mass state to a much lower mass configuration, and the agent of that change may be the growth of large planets in the system which have induced significant eccentricities in the β Pictoris disk.

5. Summary Findings and Their Implications for the Region Beyond 50 AU

Collisional evolution is an important process in the Kuiper Disk. We have employed a simple collision rate code to make an initial study of the hypothesis that the early Kuiper

Disk was much more massive than the disk's present population structure.

For the future, a more sophisticated model employing time-dependent mass and mass-coupled velocity evolution is clearly called for. As a precursor to that, however, the simple model described in §3 has been used to calculate collision rates, lower-limit growth timescales, and the other parameters in such a disk. Subject to the limitations of the simple model used here, the following findings have been made:

1. The required disk mass inside 50 AU needed to achieve QB_1 growth times of order 10^9 years or less by binary accretion from kilometer-scale seeds in the absence of significant gas drag, was found to be $35M_\oplus$ to $50M_\oplus$ for $\langle e \rangle$ greater than approximately 0.5%, and $10M_\oplus$ for $\langle e \rangle$ of 0.1%. If the mean random eccentricities in the swarm between 30 and 50 AU were indeed 0.5% or larger, then the high disk mass requirement implies that during the accretion epoch, the 30 to 50 AU zone may have contained up to several times the surface mass density of solids predicted by a simple extension of the present-day surface mass density of the solid material in the giant planets. Such a finding would be in accord the view that the formation of the giant planets in the 5 to 30 AU region was inefficient and that the 15 to 30 AU zone probably contained significantly more mass during the accretion of Uranus and Neptune than it presently does (cf., Lissauer & Stewart 1993).

2. Until growth proceeded to the ~30 km radius scale, the disk must have remained dynamically cold with a mean random eccentricity of order 5×10^{-3} or less. Eccentricities of 2–3% or higher seem implausible because they imply masses significantly exceeding 50 $M_\oplus$ in the 30 to 50 AU zone. Once the mean random eccentricity in any region exceeded the critical eccentricity for erosion for small bodies, the accretional regime becomes erosional for those objects. Because power law populations contain fewer objects at larger size scales, collisional erosion likely created a significant flattening in the disk's population power law slope below radius scales from ≈20 to ≈100 km, depending on their mechanical properties.

3. An important consequence of this change is that the mass of the disk will start to decline, thereby truncating the growth of larger objects. Therefore, although QB_1-scale objects could continue to grow in a massive disk at eccentricities in the 2-10% range (depending on their mass, mechanical properties, and heliocentric distance), the smaller objects from which they are built would be rapidly depleted on a timescale of $\sim 3 \times 10^7$ years by erosive collisions once $\langle e \rangle$ exceeded ≈1%. This process effectively depletes the small-body population in the disk, which essentially "freezes" the sizes of the QB_1-like

objects at about the scale they reached when $\langle e \rangle$ became erosive.

4. The fact that small bodies in the present-day disk exhibit a destructive erosion timescale close to the age of the Solar System (Stern 1995) is a strong indicator that the erosive mass loss process is still at work, and that the 35-50 AU zone has reached an equilibrium in the sense that the population has thinned to the point that the relevant timescale for change among small bodies equals the age of the system.

5. The fact that accretion in the 30 AU zone was arrested after Neptune grew large enough to induce erosional eccentricities there may imply a coupling of the formation time of Neptune to both the end of growth of the largest QB_1s, and the era of dramatic, erosive mass loss from the Kuiper Disk.

6. During the period of rapid mass loss following the transition to an erosive regime for kilometer-scale objects, the radial optical depth of the Kuiper Disk probably reached the 10^{-4} to 10^{-5} level, suggesting an interesting correspondence to the β Pictoris system as it appears today.

In closing, it is useful to explore the possibility that the Kuiper Disk may extend well beyond the $\approx$50 AU limit to which objects have been detected to date.

Recent dynamical studies by Duncan et al. (1995) have provided strong evidence that the role of the giant planets is negligible in exciting eccentricities beyond $\sim$50 AU. As such, the erosive mass loss that occurred in the 30-50 AU region probably never occurred outside 50 AU, and growth may have proceeded unabated to the present time (assuming internal velocity evolution never increased eccentricities beyond e^* in that region).

Given the evidence that the low surface mass density in the 30 to 50 AU zone is a consequence of erosive (and dynamical) evolution from a higher-mass state, it is natural to conclude that the primordial disk did not truncate near the limit of present detections ($\approx$50 AU).

If the disk initially extended well beyond 50 AU, then its present-day structure may resemble that shown schematically in Figure 5. Notice how the depicted disk surface mass density rises dramatically (and may even approach the primordial surface mass density) beyond $\sim$50 AU. This predicted rise in Σ is a consequence of our findings that (i) the initial mass of solids was greater by a factor of 2 to 3 than that actually accreted into the giant planets and (ii) that the eccentricities beyond $\approx$50 AU remained dynamically cold enough to inhibit extensive mass loss.

As shown in Figure 5, it is an intriguing possibility that, in the region beyond ≈50 AU (or perhaps ~ 65 AU if Malhotra's (1995) mean motion resonance sweeping mechanism was important), the initial surface mass density of solids may still be extant. Although growth times at 60-70 AU would be an order of magnitude longer than at 40 AU (see Figure 3), there appears to be time for 50-100 km radius, and conceivably larger bodies, to have accreted there.† How far out growth proceeded is not clear at this time, as shown by the dotted line in the upper panel of Figure 5 at 75 AU. However, at greater and greater distances, the role of collisions would be progressively less important as the collision time, $n\sigma v$, decreases. Therefore, at some as-yet undetermined distance, the population size structure should return to its primordial distribution, but may depend on the disk reaching quite large distances (e.g., well beyond 100 AU).

The hypothesis that the disk not only extends beyond 50 AU, but also shows an increased surface mass density beyond roughly this point, is testable. Since objects of the QB_1-class at 70 AU would only be ≈3 astronomical magnitudes fainter than the R=23-24 magnitude bodies presently being discovered inside 45 AU by 2 meter class telescopes, there is the prospect that future searches using larger (e.g., 8-10 meter class) telescopes could detect these more distant bodies. Their number density should provide a powerful constraint on the total mass of the disk beyond 50 AU, in turn providing a strong test of whether the 35-50 AU region has indeed evolved to its present state through mass loss. A second test for such a massive, distant reservoir would be its IR signature. Between 10% and 20% of the optical depth is created beyond 50 AU; the strong IR signal from this dust would peak near 90 μm, which is longer in wavelength than the IR signal from material in the 30 to 50 AU region. Any detection of this IR signature or individual objects beyond 50 AU would provide valuable constraints on the initial surface mass density and surface mass density distribution of the outer Solar System.

If the region beyond 50 AU is indeed populated with a massive disk of comets and planetesimals, one can think of the evolved, (i.e., mass-depleted), region inside ~50 AU as one where accretion was arrested at a characteristic radius scale of ≈200 km, and the more-primordial, outer region beyond 50 AU as one where accretion may still be proceeding.

---

† In fact, our models show that objects as large as several thousand kilometers in diameter could have accreted out to ~100 AU, if internal velocity evolution did not induce eccentricities that were too large.

Acknowledgements

It is a pleasure to acknowledge discussions with my colleagues Josh Colwell, Martin Duncan, Michel Festou, Hal Levison, and Paul Weissman concerning this manuscript. An anonymous referee also provided useful comments. The research reported here was supported by the NASA Origins of Solar Systems Program.

References

Alcock, C., and P. Hut, 1995. AJ, submitted.

Backman, D.E., and Paresce, F., 1993. In *Protostars and Planets III*, (E.H. Levy & J. Lunine eds.), Tucson: Univ. Ariz. Press, 1253.

Backman, D.E., A. Dasgupta, and R.E. Stencel, 1995. *ApJ*, 450, L35.

Cochran, A.L., H.F. Levison, S.A. Stern, and M.J. Duncan, 1995a. *IAUC*, 6163.

Cochran, A.L., H.F. Levison, S.A. Stern, and M.J. Duncan, 1995b. *ApJ*, 453, 342.

Cruikshank, D.P., 1994. Invited Lecture given at the International School of Space Chemistry, "Ettore Majorana" Center for Scientific Culture, Erice, Italy.

Davis, D.R., and Farinella, P., 1996. Icarus, submitted.

Davis, D.R., et al. 1989. In *Asteroids II* (R.P. Binzel, T. Gehrels, and M.S. Matthews, eds.). University of Arizona Press: Tucson, p805.

Duncan, M.J., T. Quinn, S. Tremaine, 1988. *AJ*, 94, L69.

Duncan, M.J., H.F. Levison, and S.M. Budd, 1995. AJ, 110, 373.

Edgeworth, K.E., 1949. *MNRAS*, 109, 600.

Fernández, J.A., 1980. *MNRAS*, 192, 481.

Fujiwara, A., et al., 1989. In *Asteroids II* (R.P. Binzel, T. Gehrels, and M.S. Matthews, eds.). University of Arizona Press: Tucson, p240.

Jewitt, D., and J.X. Luu, 1993. *Nature*, 362, 730.

Jewitt, D., and J.X. Luu, 1995. *AJ*, 109, 1867.

Kuiper, G.P., 1951. In *Astrophysics: A Topical Symposium* (J.A. Hynek, ed.), McGraw Hill:New York, 357.

Lissauer, J.J., and G.R. Stewart, 1993. In *Protostars and Planets III* (E.H. Levy and J.I. Lunine, eds.), Univ. Ariz. Press:Tucson, pp. 1061.

Lissauer, J.J., J.B. Pollack, , G.W. Wetherill, and D.J. Stevenson, 1996. In *Neptune and Triton* (D.P. Cruikshank and M.S. Matthews, eds.). Univ. of Arizona Press:Tucson, 37.

Malhotra, R., 1995. *AJ*, 110, 420.

Quinn, T.R., S. Tremaine, and M.J. Duncan, 1990, *ApJ*, 355, 667.

Stern, S.A. 1989, PASP, 101, 126.

Stern, S.A., 1995. *AJ*, 110, 856.

Stern, S.A., 1996. *A&A*, in press.

Tremaine, S., 1990. In *Baryonic Dark Matter* (D. Lynden-Bell and G. Gilmore, eds.). Kluwer: Norwell, MA, 37.

Weissman, P.R., 1995. *ARA&A*, 33, 327.

Weissman, P.R., and H.F. Levison, 1996. In *Pluto and Charon* (D.J. Tholen & S.A. Stern, eds.), Univ. Ariz. Press:Tucson in press.

Young, E.F., and E. Asphaug, 1995. *BAAS*, 27, 68 (abstract).

Figure Captions

Figure 1: The critical eccentricity (e*) boundary between the accretional (i.e., net mass accumulation) and erosional (i.e., net mass loss) regimes for collisions on individual objects at two representative heliocentric distances: 35 and 60 AU. Critical eccentricity curves for both strong and weak objects are shown, as a function of target radius, at each distance. The strong target case uses $\rho = 2$ g cm^{-3} and $s = 3 \times 10^6$ erg g^{-1}; the weak target case uses $\rho = 0.5$ g cm^{-3} and $s = 3 \times 10^4$ erg g^{-1}. In both cases we assume 12% of the energy of the impactor is converted to translational energy of the ejecta (cf., e.g., Fujiwara et al. 1989).

Figure 2: Estimates for the timescale to erode 2.5 km and 10 km radius objects by half their mass, as a function of their eccentricity. The disk assumed here consists of $35M_\oplus$ between 35 and 50 AU, and extends outward like R^{-2}. These timescales were estimated at 35, 45, 55, and 65 AU assuming that (i) the target bodies are mechanically strong, (ii) 12% of the energy of the accretional event was converted into translational velocity of ejecta, and (iii) the characteristic ejecta velocity is 10% of the impact velocity (cf., Davis et al. 1989; Fujiwara et al. 1989); for a complete description of this model, cf., Stern (1995). Below $\langle e \rangle = 0.01$, the erosion timescales become asymptotically longer, since the net mass eroded drops to zero at the critical eccentricity for erosion, e^*, which is of order a few parts in 10^3 (see Figure 1).

Figure 3: The two upper panels show the characteristic time for objects in the disk to double their mass as a function of their size and heliocentric distance. The disk modelled here has a total mass of $35M_\oplus$ inside 50 AU. Upper left panel: for the case $\langle e \rangle = 3 \times 10^{-3}$; upper right panel: for the case $\langle e \rangle = 2.6 \times 10^{-2}$. The two lower panels show the integrated time for objects of given size to grow from a 3 km radius seed. Lower left panel: for the case $\langle e \rangle = 3 \times 10^{-3}$; lower right panel: for the case $\langle e \rangle = 2.6 \times 10^{-2}$. Lower disk masses increase these accretion times.

Figure 4: Here we depict the results of a suite of integrated growth time calculations like those shown for two specific cases in Figure 3 to show the dependence of the growth time for QB_1-class bodies in the assumed disk mass and mean random eccentricity. The growth time estimates shown here are for objects at 35 AU. See §5.

Figure 5: Schematic depiction of the suggested present-day structure of the Kuiper Disk. In the upper panel the 30–50 AU zone is shown as both collisionally and dynamically

evolved, since dynamics acted both to destablize most orbits with a <42 AU (e.g., Duncan et al. 1995), and to induce eccentricities that induced collisions out to almost 50 AU. The dynamically and collisionally evolved zone might extend as far as $\approx$63 AU, if the suggestion by Malhotra (1995) that the sweeping of mean motion resonances generated by the migration of the giant planets during the formation of the Oort Cloud is correct. Beyond this region we expect there to be a collisionally evolved zone where accretion has occurred but eccentricity perturbations by the giant planets were too low to have initiated erosion, and beyond that, a primordial zone in which the accretion rates hardly modified the initial population of objects. In the lower panel the question-marked lines indicate possible present-day structure. No attempt is made here to depict the high-frequency structure of mass density in the 30–42 AU zone (cf., Duncan et al. 1995). Notice the surface mass density is shown to increase beyond $\approx$ 42 AU, the limit of the Neptune secular resonances that amplify eccentricities in the Kuiper Disk. The dashed line indicates the probable primordial structure. One important implication here is that the "edge" at 30 AU first noticed by Edgeworth and Kuiper may in fact represent only the inner boundary of a trough resulting from a combination of dynamical collisional evolution. Notice also that the surface mass density in the less evolved region beyond $\approx$50 AU may increase toward or even to the primordial surface mass density of solids of that region.

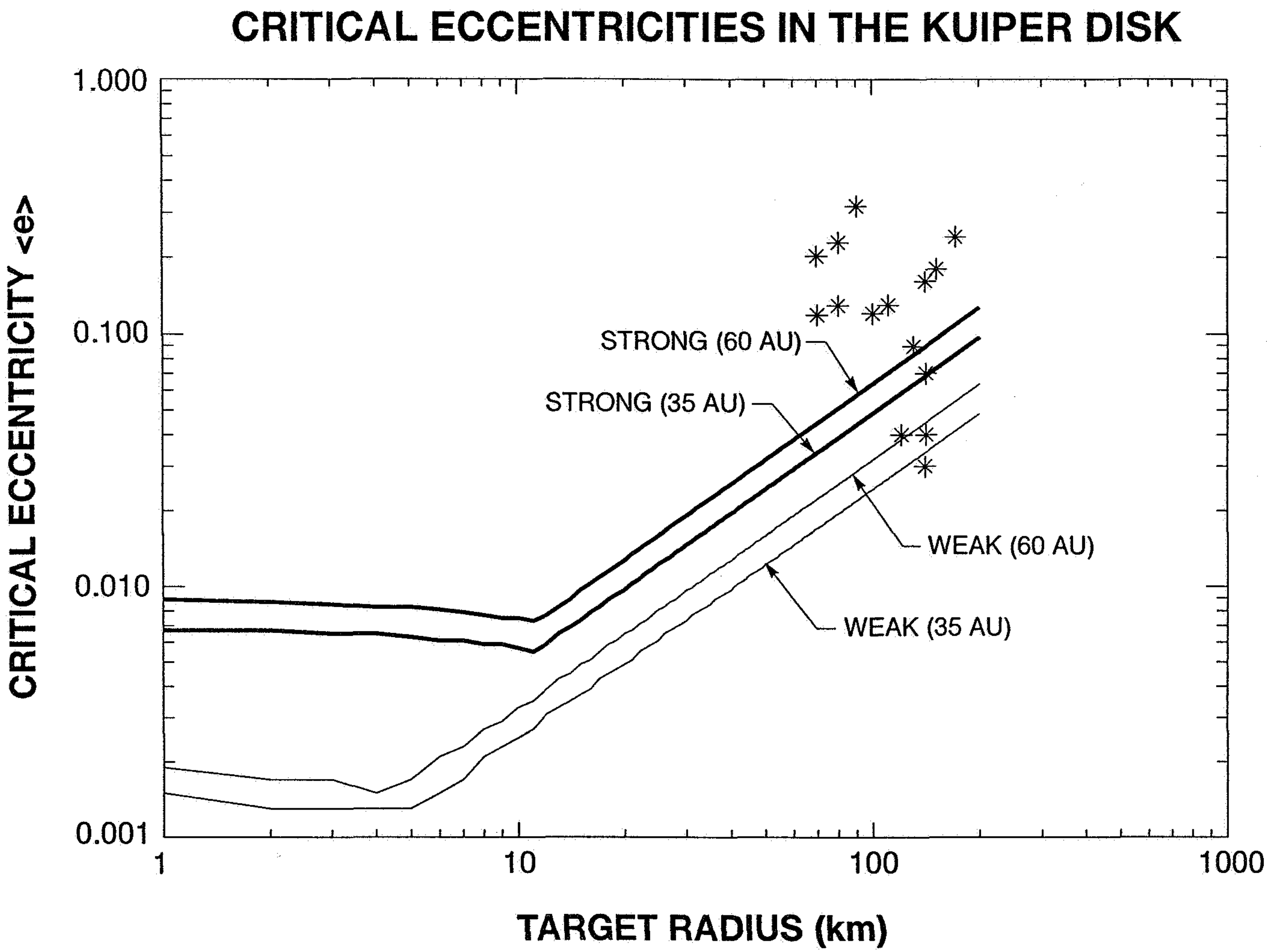

CRITICAL ECCENTRICITIES IN THE KUIPER DISK
CRITICAL ECCENTRICITY <e>
1.000
0.100
0.010
0.001
STRONG (60 AU)
STRONG (35 AU)
WEAK (60 AU)
WEAK (35 AU)
1
10
100
1000
TARGET RADIUS (km)

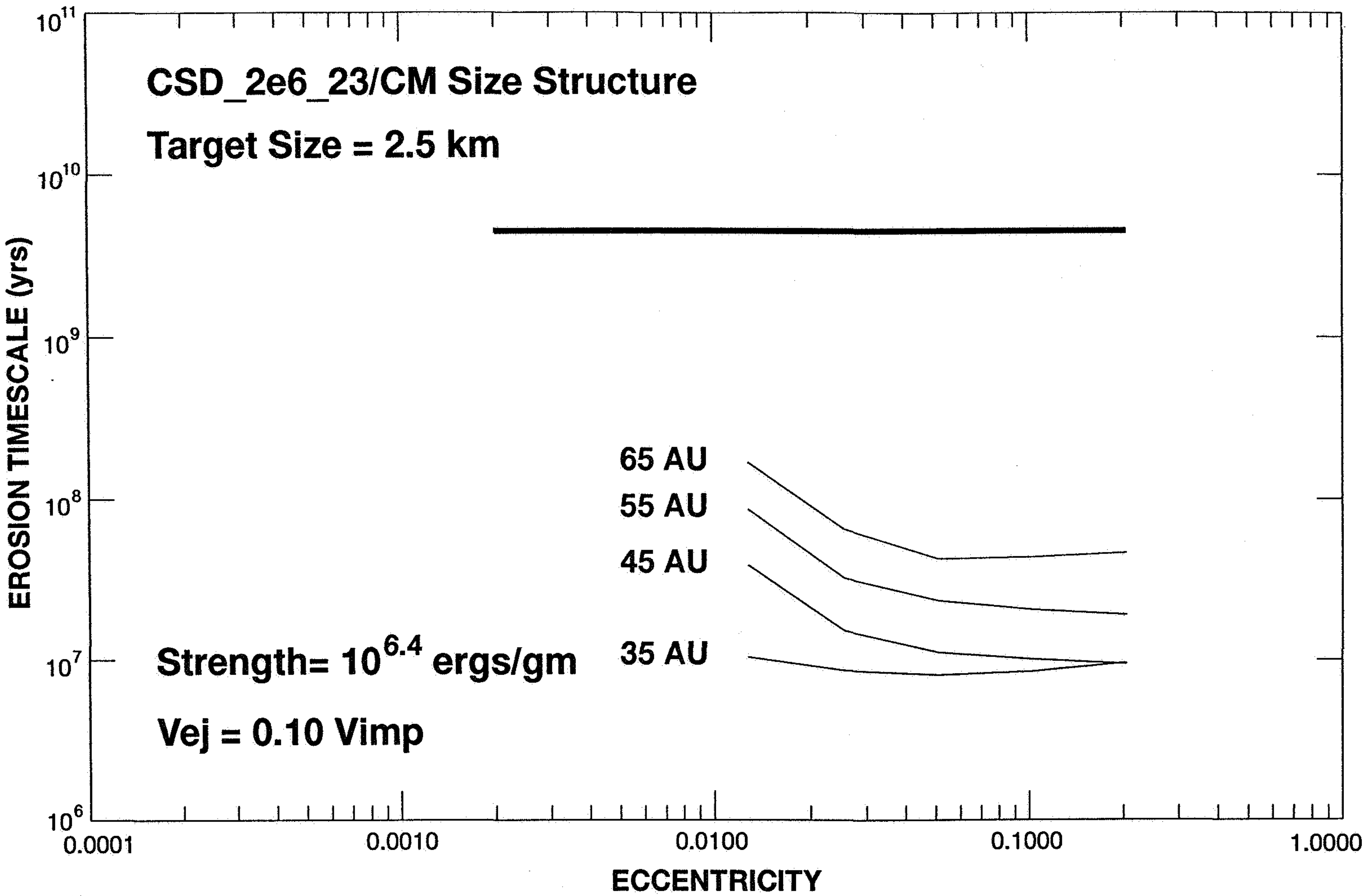
CSD_2e6_23/CM Size Structure
Target Size = 2.5 km
65 AU
55 AU
45 AU
35 AU
Strength= $10^{6.4}$ ergs/gm
Vej = 0.10 Vimp
EROSION TIMESCALE (yrs)
ECCENTRICITY
10^{11}
10^{10}
10^{9}
10^{8}
10^{7}
10^{6}
0.0001
0.0010
0.0100
0.1000
1.0000

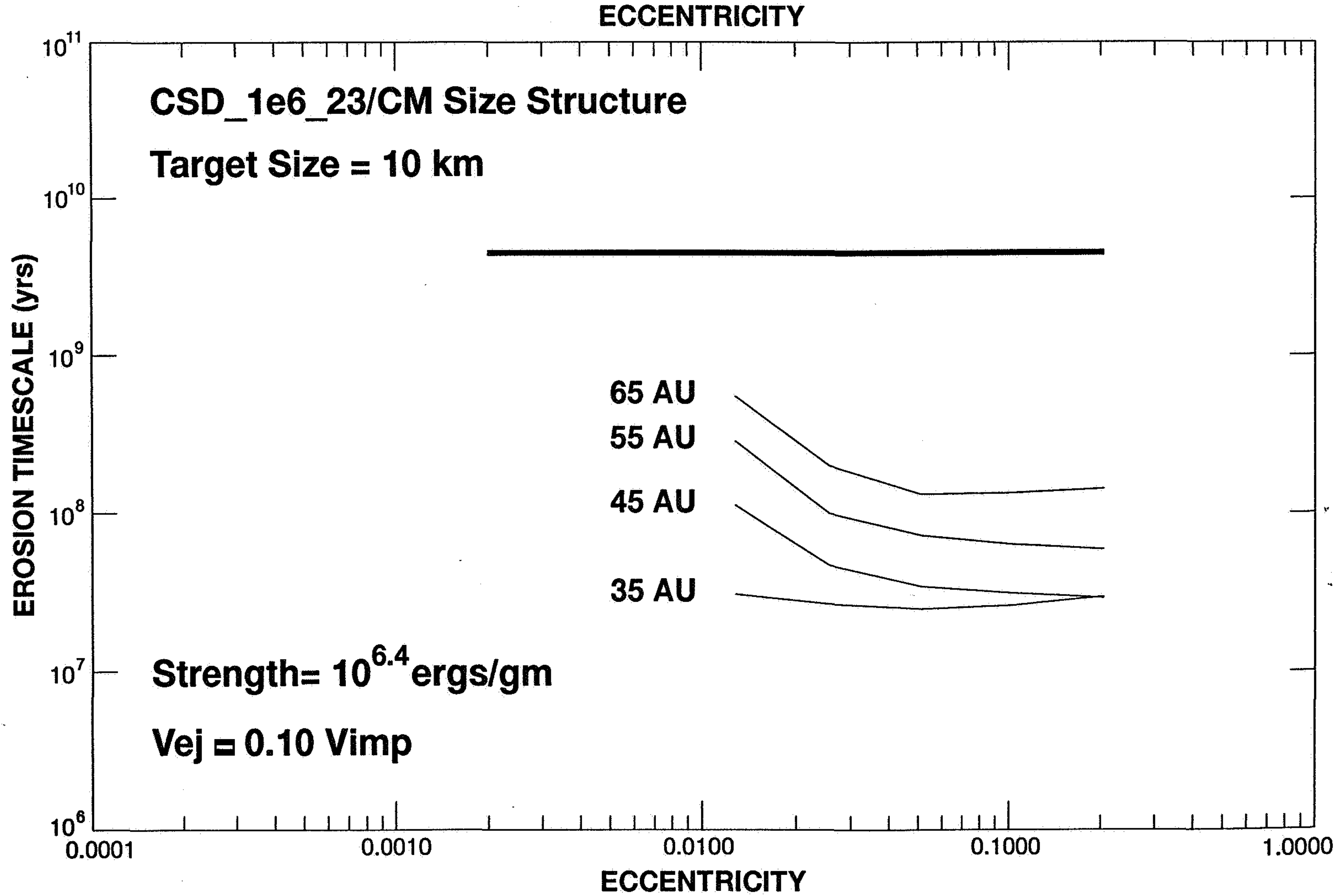
CSD_1e6_23/CM Size Structure
Target Size = 10 km
65 AU
55 AU
45 AU
35 AU
Strength= $10^{6.4}$ ergs/gm
Vej = 0.10 Vimp
EROSION TIMESCALE (yrs)
ECCENTRICITY
10^{11}
10^{10}
10^{9}
10^{8}
10^{7}
10^{6}
0.0001
0.0010
0.0100
0.1000
1.0000

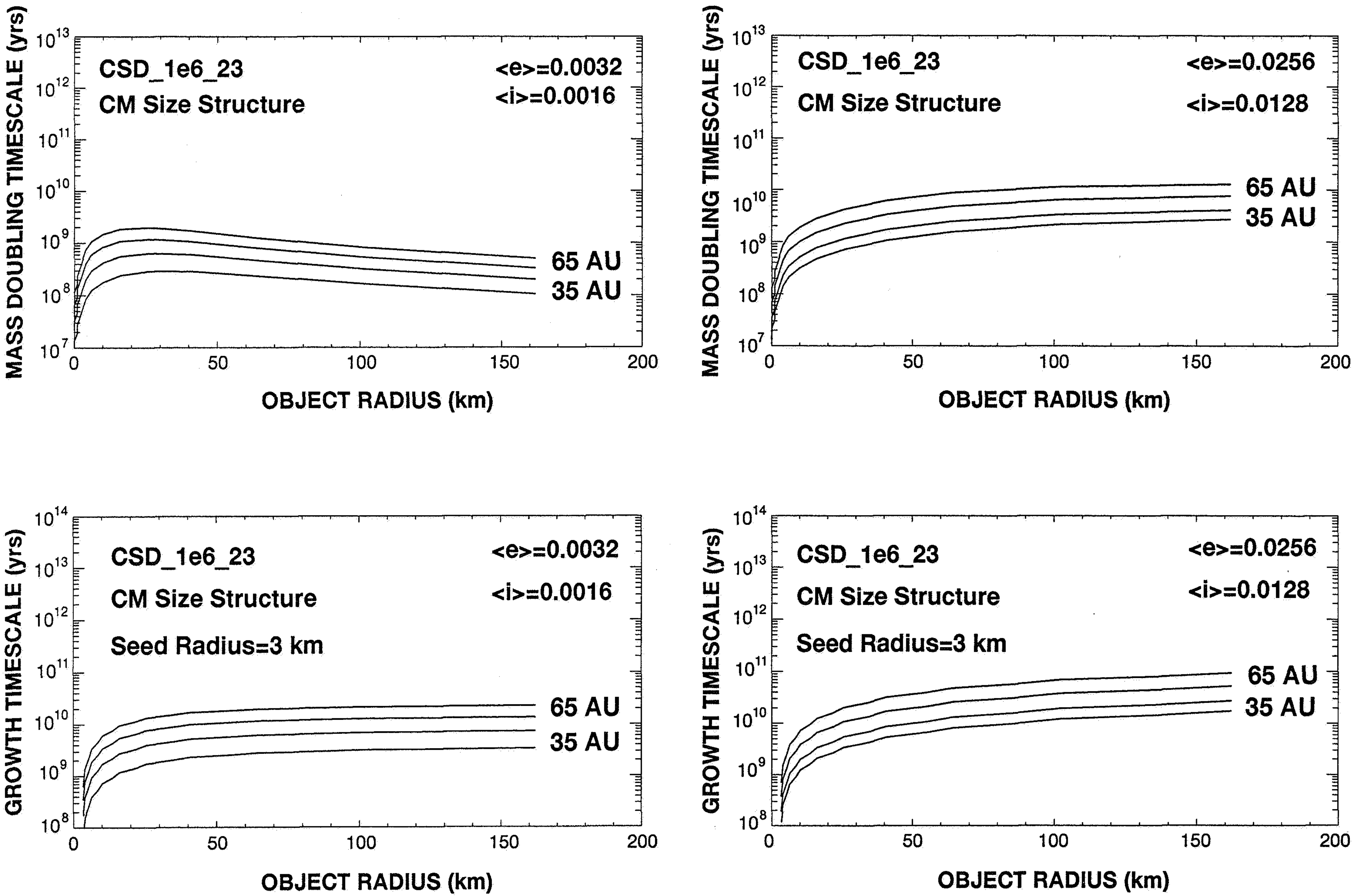
MASS DOUBLING TIMESCALE (yrs)
CSD_1e6_23
CM Size Structure
<e>=0.0032
<i>=0.0016
65 AU
35 AU
OBJECT RADIUS (km)
MASS DOUBLING TIMESCALE (yrs)
CSD_1e6_23
CM Size Structure
<e>=0.0256
<i>=0.0128
65 AU
35 AU
OBJECT RADIUS (km)
GROWTH TIMESCALE (yrs)
CSD_1e6_23
CM Size Structure
Seed Radius=3 km
<e>=0.0032
<i>=0.0016
65 AU
35 AU
OBJECT RADIUS (km)
GROWTH TIMESCALE (yrs)
CSD_1e6_23
CM Size Structure
Seed Radius=3 km
<e>=0.0256
<i>=0.0128
65 AU
35 AU
OBJECT RADIUS (km)

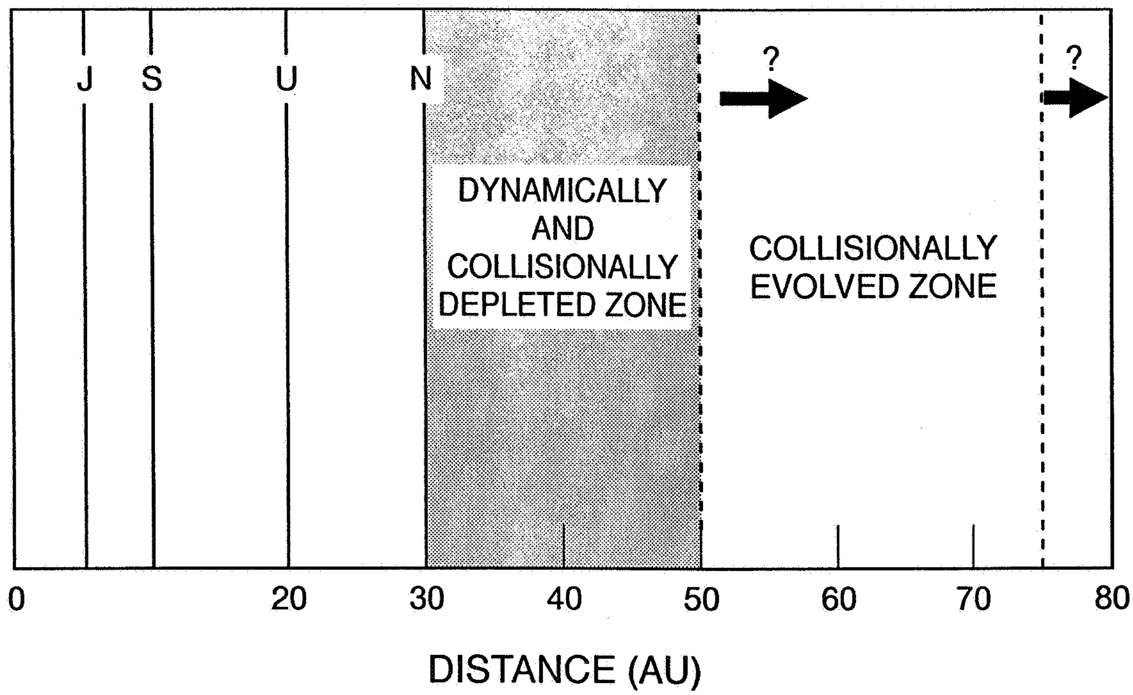

J
S
U
N
DYNAMICALLY AND COLLISIONALLY DEPLETED ZONE
?
?
COLLISIONALLY EVOLVED ZONE
0
20
30
40
50
60
70
80
DISTANCE (AU)

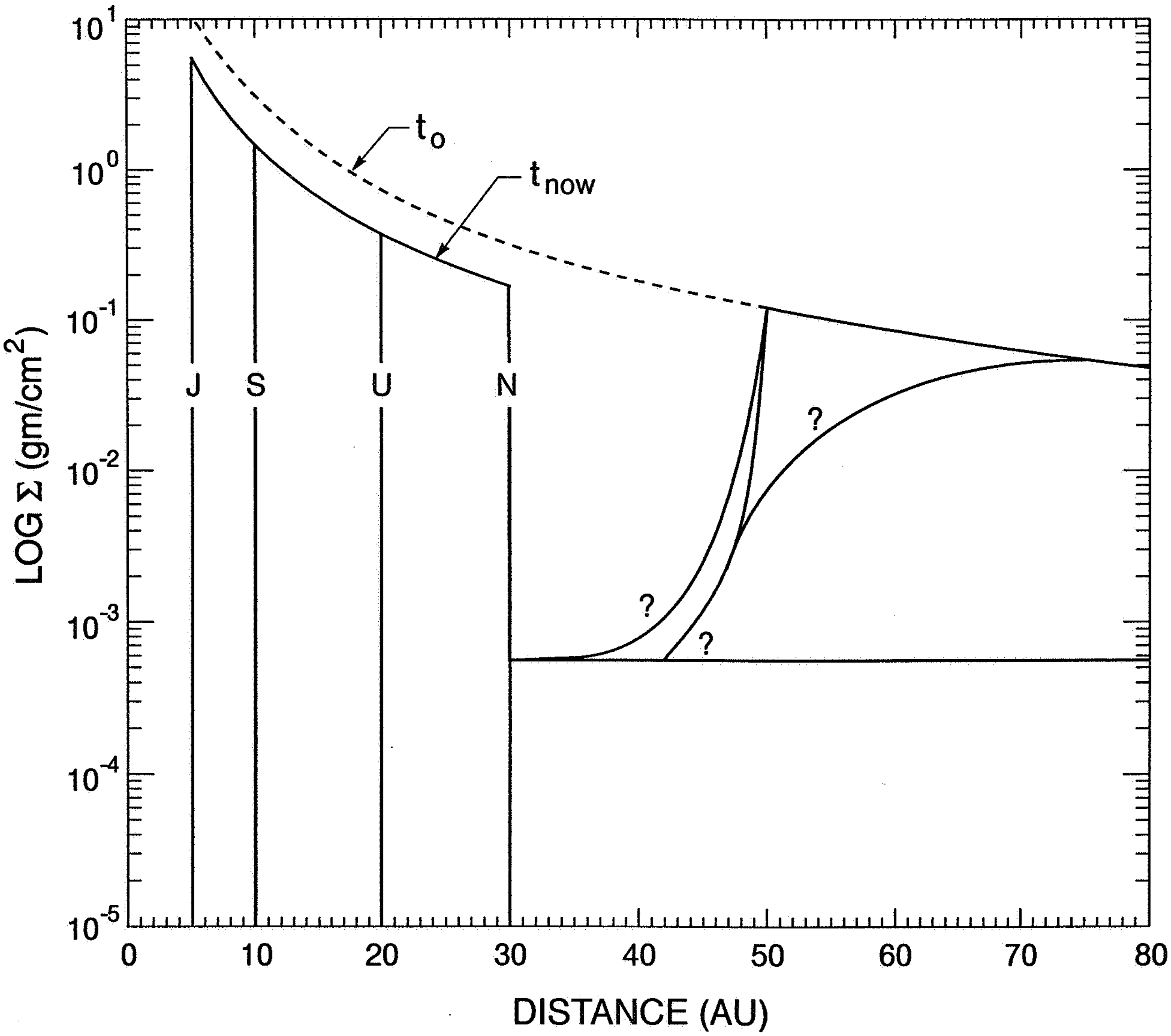

10^1
10^0
10^{-1}
10^{-2}
10^{-3}
10^{-4}
10^{-5}
LOG Σ (gm/cm^2)
t_o
t_{now}
J
S
U
N
?
?
?
0
10
20
30
40
50
60
70
80
DISTANCE (AU)

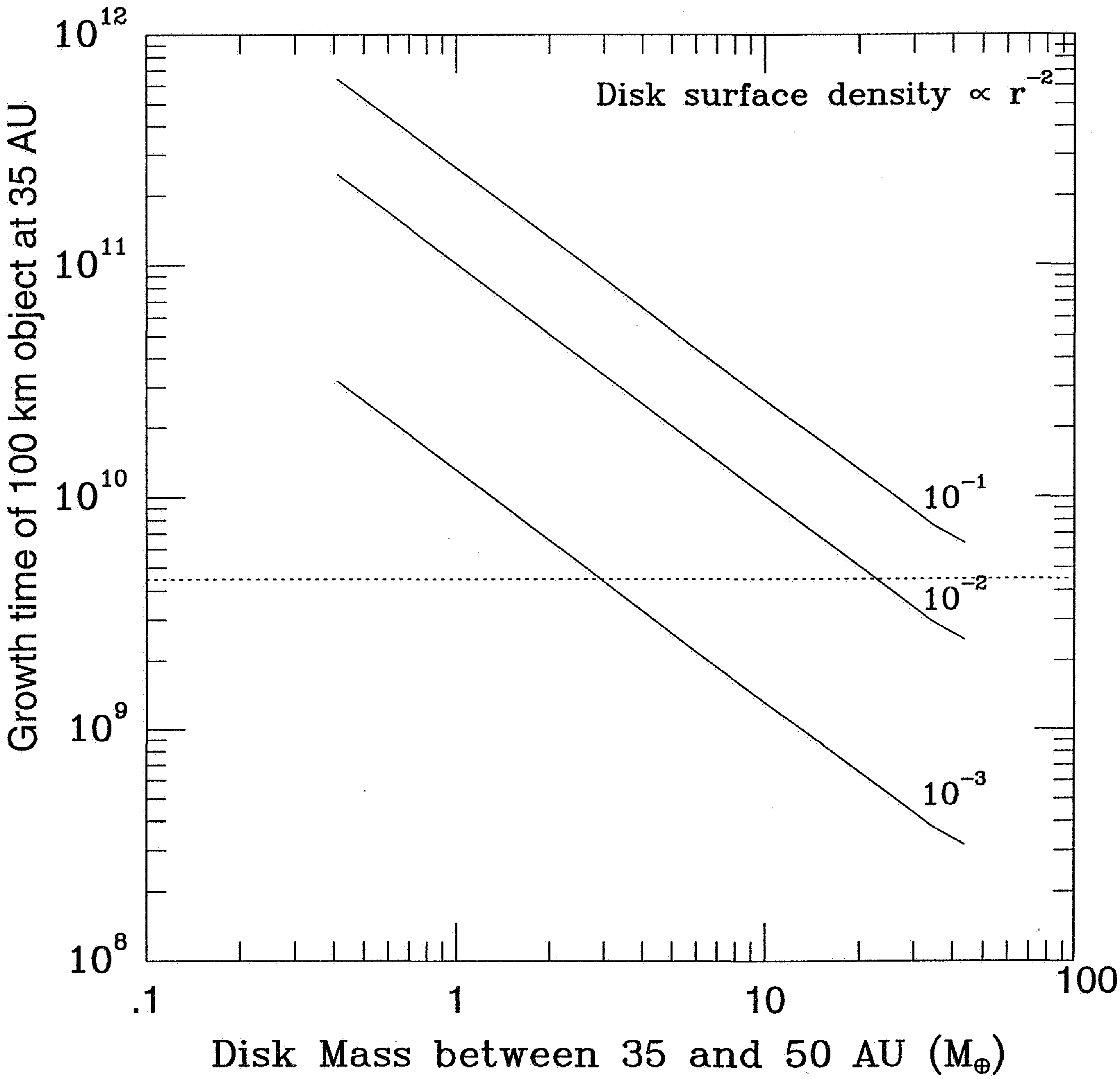

Disk surface density ∝ r^-2
10^-1
10^-2
10^-3
10^12
10^11
10^10
10^9
10^8
.1
1
10
100
Growth time of 100 km object at 35 AU
Disk Mass between 35 and 50 AU (M⊕)